Toxicology Mechanisms and Methods

ISSN: 1537-6516 (Print) 1537-6524 (Online) Journal homepage: http://www.tandfonline.com/loi/itxm20

# The aminopeptidase inhibitor, z-L-CMK is toxic and induced cell death in Jurkat T cells through oxidative stress

E. H. Yeo, W.L. Goh & S.C. Chow

**To cite this article:** E. H. Yeo, W.L. Goh & S.C. Chow (2017): The aminopeptidase inhibitor, z-L-CMK is toxic and induced cell death in Jurkat T cells through oxidative stress, Toxicology Mechanisms and Methods, DOI: 10.1080/15376516.2017.1373882

**To link to this article:** http://dx.doi.org/10.1080/15376516.2017.1373882

Accepted author version posted online: 29 Aug 2017.

# The aminopeptidase inhibitor, z-L-CMK is toxic and induced cell death in Jurkat T cells through oxidative stress

Yeo, E. H., Goh, W.L. and Chow, S.C.*

School of Science, Monash University Malaysia, Jalan Lagoon Selatan, Bandar Sunway, 46150 Selangor Darul Ehsan, Malaysia

*To whom all correspondence should be addressed: School of Science, Monash University Malaysia, Jalan Lagoon Selatan, Bandar Sunway, 46150 Selangor Darul Ehsan, Malaysia.

Email: chow.sek.chuen@monash.edu

**Abstract**

The leucine aminopeptidase inhibitor, benzyloxycarbonyl-leucine-chloromethylketone (z-L-CMK) was found to be toxic and readily induced cell death in Jurkat T cells. Dose-response studies show that lower concentration of z-L-CMK induced apoptosis in Jurkat T cells whereas higher concentration causes necrosis. In z-L-CMK-induced apoptosis, both the initiator caspases (-8 and -9) and effector caspases (-3 and -6) were processed to their respective subunits. However, the caspases remained intact in z-L-CMK-induced necrosis. The caspase inhibitor, z-VAD-FMK inhibited z-L-CMK mediated apoptosis and caspase processing but has no effect on z-L-CMK-induced necrosis in Jurkat T cells. The high mobility group protein B1 (HMGB1) protein was found to be released into the culture medium by the necrotic cells and not the apoptotic cells. These results indicate that the necrotic cell death mediated by z-L-CMK at high concentrations is via classical necrosis rather than secondary necrosis. We also demonstrated that cell death mediated by z-L-CMK was associated with oxidative stress via the depletion of intracellular GSH and increase in reactive oxygen species (ROS), which was blocked by N-acetyl cysteine. Taken together, the results demonstrated that z-L-CMK is toxic to Jurkat T cells and induces apoptosis at low concentrations, while at higher concentrations the cells die of necrosis. The toxic side effects in Jurkat T cells mediated by z-L-CMK are associated with oxidative stress via the depletion of gluthatione (GSH) and accumulation ROS.

## Introduction

Peptidyl-halomethyl-ketones were designed specifically as active site-directed irreversible protease inhibitors. They are very useful pharmacological and biochemical tools for the elucidation of molecular structure, mechanism of reaction and biological functions of serine and cysteine proteases (Angliker et al, 1987; Krantz *et al*., 1991, Powers *et al*., 2002). The peptidyl moiety of the peptidyl-halomethyl-ketones serves as the affinity group, which complement the S1 and S2 sites of the target protease (Liow and Chow, 2013). The halomethyl-ketone moiety, which contains the halide group, functions as the reactive entity that labels the enzyme. This reaction involves the expulsion of the halide group to form an irreversible thiomethylketone with the cysteine or serine residues at the active site of the enzyme (Powers *et al*., 2002).

Some of the earliest peptidyl chloromethyl ketone (CMK) serine protease inhibitors developed includes tosyl-phenylalanine chloromethyl ketone (TPCK) and tosyl-lysine chloromethyl ketone (TLCK) which were initially used to block the activity of chymotrypsin and trypsin, respectively (Schoellmann, 1962). Accumulating evidence over the years have shown that both TPCK and TLCK possess numerous side effects besides blocking serine proteases (Gillibert *et al*., 2005a, Ha *et al*., 2009, Perez-G *et al*., 2008, Weis *et al*., 1995, Kim *et al*., 1995, Gillibert *et al*., 2005b). The lack of specificity in these inhibitors maybe attributed to the highly reactive CMK moiety, which results in nucleophilic displacement and irreversible alkylation of non-target molecules indiscriminately in cells (Rauber *et al*., 1986, Shaw *et al*., 1986). More recently, we reported that the cathepsin B inhibitor, z-FA-CMK was toxic and readily induce cell

death in human primary T cells as well as the leukemic Jurkat T cells (Liow and Chow, 2013; Rajah and Chow, 2015). We also observed that benzyloxycarbonyl-alanine-chloromethylketone (z-A-CMK), an analog of z-FA-CMK exhibit similar toxicity in Jurkat T cells (Liow and Chow, 2013). Peptidyl-CMK with alanine in the P1 position (A-CMK) was originally developed to block leucine aminopeptidase, one of the many aminopeptidases that are involved in protein maturation, degradation and regulation of hormonal and non-hormonal peptides (Birch et al, 1972). Another potent inhibitor designed to block this aminopeptidase is L-CMK with leucine at the P1 position, and both were also effective inhibitors for amino acyl-tRNA synthetases (Birch et al, 1972).

In view of their similar mechanism of action on amino peptidases and amino acyl tRNA synthetases (Birch et al, 1972), we examined whether z-L-CMK possess any toxic side effects in Jurkat T cells as seen with z-A-CMK (Liow and Chow, 2013). Similar to z-A-CMK, we found z-L-CMK toxic and readily induced cell death in a time- and dose-dependent manner in Jurkat T cells. Cells treated with lower concentrations of z-L-CMK were found to undergo apoptosis whereas the cells die of necrosis when exposed to higher concentrations of the peptidyl CMK. The caspase-inhibitor, z-VAD-FMK inhibits apoptotic cell death and caspase processing induced by low concentration of z-L-CMK in Jurkat T cells, but has no effect on necrosis mediated by high concentration of the peptidyl-CMK. The released of high mobility group protein B1 (HMGB1) protein into the culture medium by necrotic cells induced by high concentrations of z-L-CMK suggests that the cells die via necrosis instead of secondary necrosis. We also observed that z-L-CMK treatment leads to depletion of intracellular GSH and accumulation of ROS in

Jurkat T cells and that cell death induced by z-L-CMK was abrogated by NAC. Collectively, these results suggest that z-L-CMK toxicity is mediated via oxidative stress.

## Materials and Methods

### *Reagents*

Benzyloxycarbonyl-valine-alanine-aspartic acid-(O-methyl)-fluoromehylketone (z-VAD-FMK), and benzyloxycarbonyl-leucine chloromethylketone (z-L-CMK) were purchased from Bachem (Switzerland). Rabbit antibodies to caspase-3 and caspase-2, and goat antibodies to caspase-8 were obtained from Santa Cruz Biotechnology (USA). Rabbit polyclonal antibodies to caspase-6 and caspase-9 were from Cell Signaling (USA). Mouse monoclonal antibody to PARP-1 was from Enzo Life Sciences (USA). RPMI 1640 and FCS were from Gibco (USA), and Hoechst 33358 and tetramethylrhodamine ethyl ester (TMRE) was from Molecular Probes (USA). Chelex®100 resin was from BioRad (USA). N-acetyl cysteine (NAC), monochlorobimane (MCB) and dihydroethidium (DHE) were obtained from Sigma Aldrich (USA).

### *Cell culture and treatments*

The human leukemic T lymphocyte cell line, Jurkat, clone E6-1 was obtained from ATCC (Rockville, MD, USA). Cell cultures were maintained in logarithmic growth phase with RPMI-1640 supplemented with 10% FCS and 2mM L-glutamine in a humidified incubator at 37°C with 5% $CO_2$ in air. For treatments, Jurkat T cells ($1x10^6$ cells/ml) were incubated with various concentrations of z-L-CMK where indicated at 37°C in an

incubator with 5% $CO_2$ in air. At time points where indicated, the treated cells were assessed for cell viability, apoptosis or prepared for western blot analysis.

***Cell viability assay***

Cell viability was determined using the CellTiter 96® AQueous One Solution Cell Proliferation Assay (MTS) as previously described (Johnson *et al*., 2000). Briefly, after treatments where indicated, aliquots of 100µl Jurkat T cell suspension ($1x10^5$ cells) were transferred to wells in a 96-well flat-bottomed tissue culture plate followed by the addition of 20µl freshly prepared MTS/PMS solution. The plate was incubated at 37°C in an incubator with 5% $CO_2$ in air for 2h before reading the absorbance at 490nm using a Tecan 200 ELISA plate reader. All samples were assayed in triplicate.

***Annexin V-FITC binding assay***

Following treatments, Jurkat T cells ($1x10^6$ cells) were washed and resuspended in 100µl of ice-cold annexin V binding buffer. The cells were incubated with 5µl each of annexin V-FITC and PI on ice in the dark for 15min. Following incubation, 400µl binding buffer was added to the cells prior to flow cytometry analysis using a FACS Calibur flow cytometer (Becton Dickinson). Excitation wavelength 488nm (FL-1 channel) for annexin V-FITC and 595nm (FL-2 channel) for PI were used for sample analysis.

***Detection of inner mitochondrial membrane potential (MMP) using flow cytometry***

Following treatments, Jurkat T cells were washed with ice-cold PBS and incubated with 0.1µM TMRE at room temperature in the dark for 15min. Cells were subsequently washed twice using ice-cold PBS and resuspended in 1ml PBS prior to flow cytometry (FACS Calibur, Becton Dickinson) analysis using excitation wavelength 595nm (FL-2 channel). The changes in MMP are reflected by the relative decrease in TMRE fluorescence intensity.

***UV fluorescence microscopy***

Nuclear morphological changes in Jurkat T cells during apoptosis were examined using UV microscopy as previously described by using Hoechst 33342 (Johnson *et al*., 2000). Following treatments, Jurkat T cells were washed with PBS before fixing in 50µl paraformaldehyde (4%) for 30min at room temperature. The fixed cells were stained with 50µl Hoechst 33342 (2.5µg/ml) for 30min and centrifuged down. The cell pellets are then resuspended in glycerol/PBS (50:50 v/v) before mounting onto slides and viewed using an Olympus fluorescence microscope (Model BX51). Apoptotic cells were identified based on morphological hallmarks such as nuclei condensation and/or nuclear fragmentation into apoptotic bodies.

***Oligonucleosomal DNA fragmentation analysis***

DNA fragmentation during apoptosis was visualized using agarose gel electrophoresis as previously described by (Liow and Chow, 2013). Following treatments, $2x10^6$ cells (live and dead) were harvested by centrifugation and resuspended in 500µl Chelex®100

resin in solution (5% v/v) with proteinase K (2.5mg/ml) and incubated at 55°C for 45min. After centrifugation at 10,000rpm for 10min, the supernatant containing the cellular DNA was collected and 2µg of DNA was mixed with loading buffer and analyzed using a GelRed™ precast 2% agarose gel. Electrophoresis was performed at 100V for 1h followed by DNA visualization using the Bio-Rad gel imaging system (Gel Doc™ EZ Imager) under UV illumination.





***Measurement of caspase-3 activity***

Caspase-3 activity in Jurkat T cells was determined using the synthetic fluorescent substrate, Ac-DEVD-AFC. Following treatments, Jurkat cells were washed with PBS and resuspended in 25µl lysis buffer (0.1M NaCl, 1mM Tris-HCl at pH7.6, 1mM EDTA, 1% Triton-X-100, 1mM PMSF). The cell suspension was taken through 3 freeze-thaw cycles using liquid nitrogen. The protein concentration of the cell lysates was measured using the Bradford Protein Assay and 30µg of protein was used to determine the caspase-3 activity. The assay was performed in final concentration of 100µM substrate in 20mM HEPES, 10% glycerol and 10mM DTT. The fluorescence changes were measured following incubation at 37°C for 15 min using a Tecan 200 ELISA plate reader at 400nm excitation wavelength and 595nm emission wavelength.

***Western blotting***

Briefly, following treatments, Jurkat cells ($2x10^6$) were lysed and protein concentration determined. Protein (30 µg) from whole-cell lysates was diluted in loading buffer (2% SDS, 10% glycerol, 50mM Tris-HCl pH 6.8, 0.2% bromophenol blue and 100mM DTT

and 4M Urea for PARP analysis) and resolved using 13% SDS-PAGE. The separated proteins were transferred onto Hybond C membrane (Amersham, UK) and probed for caspase-2, -3, -6, -8, -9, PARP and β-actin using antibodies. Detection was performed using appropriate secondary antibodies conjugated to horseradish peroxidase followed by chemiluminescence (Amersham) and visualized using a chemiluminescence western blot scanner (LI-COR C-DiGit).





***Determination of intracellular GSH levels***

The intracellular GSH levels in Jurkat T cells was determined as described by (Kamencic *et al*., 2000). Following treatments, Jurkat T cells ($1x10^5$) were centrifuged at 3500rpm for 10min and washed with 100µl of PBS before resuspended in 100µl of MCB (100µM) in PBS. The unbound MCB is non-fluorescent but forms a highly blue fluorogenic adduct when bound to GSH. The fluorescence intensity was measured following incubation at 37°C for 30min in the dark, at excitation wavelength of 390nm and emission wavelength of 460nm using a Tecan 200 ELISA plate reader. Complete media with MCB was used as background fluorescence control.

***Measurement of ROS accumulation in Jurkat T cells***

The production and intracellular accumulation of ROS in Jurkat T cells was detected using DHE, a redox sensitive fluorogenic probe that reacts with superoxides to form 2-hydroxyethidium, a red fluorescent product which intercalates with nuclear DNA (Owusu-Ansah *et al*., 2008). Following treatments where indicated, Jurkat T cells were washed and resuspended in 500µl serum-free RPMI medium and incubated with 10µM

DHE at 37°C in the dark for 30min. Cells were subsequently washed twice using ice-cold PBS and resuspended in 500µl PBS prior to flowcytometry analysis (FACS Calibur, Becton Dickinson) using excitation wavelength 518nm (FL-2 channel).

***Dot-blot detection of HMGB1 protein in Jurkat T cell culture supernatants***

The release of HMGB1 protein form Jurkat T cells following treatments was determined using dot-blot analysis. Following treatments, the Jurkat T cell culture supernatants were collected and centrifuged at 1500rpm for 15min at 4°C for 10min. Aliquots of 100µl of culture supernatants were loaded into wells of the dot blot apparatus. The culture supernatants (100µl) were filtered onto Hybond C membrane (Amersham UK) using vacuum suction. The membrane was subsequently probed with antibodies to HMGB1 followed by HRP-conjugated secondary antibodies before chemiluminescence (Amersham) detection and visualization using chemiluminescence western blot scanner (LI-COR C-DiGit).

**Statistical analysis of the data.** All the experimental data was analyzed using Graph-pad PRISM version 6.04 (GraphPad Software, San Diego, California, USA). Results shown represent mean ± SEM where statistical comparison between treatment groups was performed using one-way ANOVA followed by Post-hoc Dunnett's Test. The statistical p value of $< 0.05$ is regarded as statistically significant.

## Results

### z-L-CMK induced cell death in Jurkat T cells in a dose- and time-dependent manner.

We have shown previously that z-A-CMK, an aminopeptidase inhibitor was toxic and readily induced cell death in Jurkat T cells (Liow and Chow, 2013). In the present study, the toxicity of another aminopeptidase inhibitor, z-L-CMK on Jurkat T cells was examined. As shown in Figure 1, z-L-CMK was toxic to Jurkat T cells and readily induced cell death in a dose- and time-dependent manner. Cell death mediated by z-L-CMK was apparent at ~10μM after 2h and higher concentration (100μM) induced a marked decrease in viability with only ~13% Jurkat T cells remained viable after 2h. At longer time points there was a marked decreased in the IC50 as shown by the shifting of the dose-response curve to the left (Figure 1).

### Cell death induced by z-L-CMK involves the externalization of PS.

One of the early hallmark of apoptotic cell death involves the externalization of PS from the inner leaflet of the cell membrane, which can be detected using annexin V-FITC labeling (van Engeland *et al*., 1998, Zhang *et al*., 1997). To determine whether cell death induced by z-L-CMK involved apoptosis, Jurkat T cells were treated with various concentrations of z-L-CMK for 6h and the binding of annexin V-FITC and uptake of PI determined using flow cytometry. As shown in Figure 2, the percentage of normal cells (annexin-FITC negative and PI negative) was found to decrease markedly with increasing concentration of z-L-CMK. Interestingly, z-L-CMK induced a transient increase in apoptotic cells (annexin V-FITC positive and PI negative) which peaks at

about 12.5μM and decreased as the concentration of z-L-CMK increases. In sharp contrast, z-L-CMK dose-dependently induced an increased in late apoptotic/necrotic cells (annexin V-FITC positive and PI positive). The results suggest that apoptosis was apparent at low concentrations of z-L-CMK (<12.5μM), but at higher concentrations (>12.5μM), a marked decrease in apoptotic cells was observed. This was accompanied by an increase in cells that may have undergone necrosis. Taken together, these results suggest that z-L-CMK induced apoptosis at low concentrations and necrosis at higher concentrations.

**Cell death in Jurkat T cells mediated by z-L-CMK is associated with the collapse of MMP.**

It is well established that the collapse of the MMP is an early event that precede the externalization of PS during apoptosis (Ding *et al*., 2000). As the MMP decreases, cytochrome C from the mitochondrial inner membrane space leaks out into the cytosol. In the presence of cytosolic ATP, cytochrome C interacts with caspase-9 to form the apoptosome, which in turn will activate caspase-9 and initiate the intrinsic apoptotic pathway (Fulda and Debatin, 2006, Hengartner, 2000). To this end the effect of z-L-CMK on Jurkat T cell MMP was examined. Jurkat T cells were treated with 10 and 50μM of z-L-CMK and at various time points the treated cells were incubated with TMRE prior to flow cytometry analysis. As illustrated in Figure 3, 10μM z-L-CMK-induced a time-dependent decrease in the MMP in Jurkat T cells. The loss of MMP was apparent after 1h and by 6h the cells have lost more than 50% of their MMP. In sharp

contrast, the MMP in cells treated with 50μM z-L-CMK was markedly reduced within 1h and no further changes seen after 6h.

**Nuclear morphological changes in Jurkat T cells treated with z-L-CMK.**

Apoptotic cells display classical nuclear morphological changes such as nuclei shrinkage and chromatin condensation as well as formation of apoptotic bodies. To further determine whether z-L-CMK-induced cell death is via apoptosis, the nuclear morphology of treated Jurkat cells was examined using UV microscopy following staining with Hoechst 33342 dye. As illustrated in Figure 4A, untreated Jurkat cells displayed normal nuclei morphology. However, Jurkat cells treated with z-L-CMK (10μM) do not display the normal nuclear morphology as control cells (Figure 4B). Instead the treated cells displayed atypical nuclei morphology with numerous cavities which is neither normal nor apoptotic nuclei morphology. These nuclear morphological changes are distinct and different from the condensed nuclear chromatin characteristic of apoptosis or fragmented apoptotic nuclei as seen in staurosporine-treated Jurkat T cells which are hallmarks of apoptotic cell death (Figure 4C). Following treatment with 10μM z-L-CMK ~90% of the treated cells displayed the distinct nuclei morphology, compared to control cells which exhibit mainly normal nuclei (94%). In contrast, 89% of staurosporine-treated Jurkat T cells (positive control) have condensed apoptotic nuclei morphology. Since the distinct nuclear morphological change in z-L-CMK is different from the classical apoptotic nuclei, we examined whether the chromatin would be cleaved into internucleosomal fragments, another hallmark of apoptotic cells. As illustrated in Figure 4D, only chromatin from staurosporine-treated cells have DNA

laddering, whereas both control and z-L-CMK treated cells have no DNA laddering, indicating that the nuclear chromatin in z-L-CMK-treated cells remained intact and have not been cleaved to the oligonucleosomal fragments.

**Role of caspases in z-L-CMK-induced cell death in Jurkat cells.**

Since the activation of caspases-3 is a critical mediator for the downstream execution of apoptosis (Degterev *et al*., 2003), the caspase-3 activity in these cells was determined. Jurkat T cells were treated with various concentrations of z-L-CMK or 1μM staurosporine (positive control) for 6h and their caspase-3 activities determined using the caspase-3 substrate, Ac-DEVD-AFC. As illustrated in Figure 5A, the cell lysates from control cells which has little or no apoptotic cells has low caspase-3 activity, whereas staurosporine-treated cells showed marked increased in caspase-3 activity. Interestingly, z-L-CMK treatment induced a transient increased in caspase-3 activity in Jurkat T cells as the concentration of z-L-CMK increases. The increased in caspase-3 activity peaked at 6.25μM z-L-CMK, which gradually reduced to below that of the control cells at 50 and 100μM. The caspase-3 activity induced by z-L-CMK correlates well with the annexin V-FITC results (Figure 3), suggesting that z-L-CMK induces apoptosis at low concentration whereas higher concentration causes necrosis. Because caspase-3 activity was activated in Jurkat T cells treated with 10μM of z-L-CMK, the effect of the caspase inhibitor z-VAD-FMK was examined. To this end, Jurkat T cells were incubated with various concentrations of z-VAD-FMK for 30min prior to treatment with 10μM and 50μM of z-L-CMK. As shown in Figure 5B, z-VAD-FMK (25-100μM) dose-dependently inhibited cell death in Jurkat T cells mediated by 10μM z-L-CMK indicating that

caspases were indeed activated in these cells and that these cells were undergoing apoptotic cell death. In sharp contrast, z-VAD-FMK has no effect on cell death mediated by 50μM z-L-CMK in Jurkat T cells (Figure 5C). These results confirmed that cells treated with high concentration of z-L-CMK were undergoing necrosis, which correlate with the annexin V-FITC binding results (Figure 3) and the lack of caspase-3 activity (Figure 5A).

**Processing and activation of caspases during z-L-CMK-induced cell death in Jurkat T cells**

Our results suggest that caspases are activated only in Jurkat T cells treated with 10μM and not with 50μM of z-L-CMK. We next examined the caspases activated in Jurkat T cells exposed to 10μM or 50μM of z-L-CMK using western blotting. As shown in Figure 6, all the caspases (-2, -3, -6, -8 and -9) examined remained intact in their pro-form in control untreated cells. Following treatment with 10 μM z-L-CMK there was a marked reduction of these pro-form caspases in Jurkat T cells. The pro-form of the initiator caspases (-2, -8 and -9) were markedly reduced, where caspase-8 and caspase-9 were cleaved into their p43/41 and p37/35 subunits, respectively. On the other hand, effector caspases, such as caspase-3 was processed to the catalytically active p17 subunit while the pro-form of caspase-6 was markedly decreased. The caspase-3 substrate, PARP (116kDa) was cleaved to the 85kDa fragment. In the presence of 50μM z-VAD-FMK, the processing of caspase-3, caspase-6 and caspase-8 was inhibited whereas processing of caspase-2 and caspase-9 was only partially blocked. The cleavage of PARP was also completely abrogated in the presence of z-VAD-FMK. Collectively,

these results demonstrated that cell death mediated by low concentration of z-L-CMK is caspase-dependent and via apoptosis. In sharp contrast, the processing of caspases and PARP in Jurkat T cells exposed to 50μM of z-L-CMK remained intact in the absence or presence of z-VAD-FMK.

**The effect of high concentration of z-L-CMK treatment on the release of HMGB1 in Jurkat T cells.**

Since all the evidence suggested that high concentration of z-L-CMK-induced direct necrosis rather than secondary necrosis following apoptosis in Jurkat T cells, we examined the release of the HMGB1 protein from these cells. HMGB1 is a DNA binding protein found in the nucleus and is only released during necrosis but not from cells undergoing secondary necrosis (Oppenheim and Yang, 2005, Taylor *et al*., 2008). Following treatments with various concentrations of z-L-CMK for 6h, the culture supernatants were collected and probed for the presence of HMGB1 using dot blot. As depicted in Figure 7A, the supernatant from control cells have little HMGB1 protein while the supernatant from freeze-thawed (FT) cells (positive control for necrosis) has a large amount of HMGB1 protein. Following treatments with increasing concentrations of z-L-CMK there was no increase in HMGB1 protein in the supernatants from cells exposed to low concentrations (up to 12.5μM). However, as the concentration of z-L-CMK increases above 12.5μM, a gradual increased in HMGB1 protein in the culture supernatants was observed (Figure 7B). The release of HMGB1 into the culture supernatants from cells treated with high concentration of z-L-CMK (<12.5μM) correlates with the induction of necrosis (Figure 3). These results confirmed that cell

death mediated by high concentration of z-L-CMK in Jurkat T cells is via necrosis and not secondary necrosis.

**z-L-CMK induced cell death is blocked by NAC.**

We have recently reported that the peptidyl methylketones such as z-VAD-FMK and z-FA-FMK were capable of inducing oxidative stress in activated T cells via the depletion of intracellular GSH and increase in ROS production (Rajah and Chow, 2014, Rajah and Chow, 2015). We therefore examined whether z-L-CMK toxicity also involves oxidative stress. To this end Jurkat T cells were treated with various concentrations of z-L-CMK in the presence of 1mM NAC. As illustrated in Figure 8, cell death induced by z-L-CMK up to 100μM was inhibited by the presence of NAC, suggesting that oxidative stress is involved. To corroborate this, we determined the intracellular GSH and ROS levels in z-L-CMK-treated cells. As shown in Figure 9A, z-L-CMK (10μM and 50μM) induced a rapid depletion of intracellular GSH levels in treated Jurkat T cells. At 10μM z-L-CMK, ~45% intracellular GSH in the treated cells were depleted within the first hour and >90% after 6h, whereas at 50μM, ~90% of the intracellular GSH in the treated cells were depleted within 1h. This rapid depletion of intracellular GSH in z-L-CMK-treated cells was accompanied by a corresponding increase in ROS accumulation (Figure 9B). At 10μM z-L-CMK, ROS accumulation in treated Jurkat T cells reaches ~4 fold above control after 6h. In the presence of 50μM z-L-CMK, the increased in ROS reached ~5 fold within 2h. Collectively, these results suggest that z-L-CMK-induced cell death involves oxidative stress through the depletion of GSH and generation of ROS.

## Discussion

We have previously shown that the cathepsin B inhibitor, z-FA-CMK was toxic and induced cell death in Jurkat T cells (Liow and Chow, 2013). Structure activity studies revealed that z-A-CMK; an analog of z-FA-CMK having the phenylalanine in the peptide sequence moiety removed was equally toxic. N-protected A-CMK was developed as an inhibitor to block the activity of leucine aminopeptidase, one of many aminopeptidases that play important roles in the regulation of protein maturation, degradation and regulation of hormonal and non-hormonal peptides (Birch et al, 1972). In the present study, we found that z-L-CMK; another leucine aminopeptidase inhibitor was also toxic and induced cell death in Jurkat T cells in a dose- and time-dependent manner.

Using several apoptosis hallmarks to distinguish apoptotic cell death from necrosis, our results showed that z-L-CMK at low concentrations readily induced apoptosis in Jurkat T cells. However, when exposed to higher concentrations of z-L-CMK, the cells die of classical necrosis. Although apoptotic cell death in Jurkat T cells mediated by z-L-CMK displayed some distinctive apoptotic features, such as the externalization of PS, collapse of MMP and activation of caspases, there was no nuclear condensation or nuclear fragmentation into apoptotic bodies in the treated cells. Instead the nuclei of the treated cells appeared convoluted and creased which are similar to our previous reports showing apoptotic cell death in the absence of nuclear condensation or DNA fragmentation (Johnson et al, 2001; Liow and Chow, 2013). It is well established that during apoptosis the activation of caspase-3 is associated with downstream activation of the DNA fragmentation factor (DFF), which exist as a complex consisting of a 40kDa

(DFF40) and a 45kDa (DFF45) subunit (Liu et al, 1997; Enari et al, 1998). Upon activation by caspase-3, DFF45 is cleaved and release DFF40, which translocate into the nucleus (Sakahira et al, 1998; Wolf et al, 1999). DFF40 contains intrinsic nuclease activity and cleaves nuclear chromatin into the hallmark apoptotic feature of oligonucleosomal-length DNA fragmentation (Liu et al, 1997). The marked increase in caspase-3 activity and cleavage of PARP in cells treated with low concentration of z-L-CMK suggests that the activity of processed caspase-3 in these cells were not blocked. Although z-L-CMK-treated cells have no DNA fragmentation or apoptotic bodies, cell death and other apoptotic hallmarks were completely abrogated by the broad spectrum caspase inhibitor z-VAD-FMK. Collectively, these results suggest that z-L-CMK may have also inhibited downstream events of apoptosis besides activating the caspase-dependent apoptotic cell death pathway in Jurkat T cells.

In contrast, Jurkat T cells treated with high concentration of z-L-CMK has no apparent apoptotic hallmarks indicating that the cells die of necrosis. Interestingly, some caspase-3 and caspase-9 were cleaved to their subunits but there was no evidence of caspase-3 activity detected and PARP was not cleaved. The presence of z-VAD-FMK has virtually no effect on cell death mediated by high concentration of z-L-CMK in these cells, although both caspase-3 and caspase-9 cleavage were attenuated. This suggests that some caspase-9 may have been activated in Jurkat T cells when treated with high concentration of z-L-CMK, and the activated caspase-9 managed to cleave some of the caspase-3. The lack of any caspase-3 activity could be due to the incomplete processing of caspase-3 to the p17 and p20 fragments. Necrotic cell death in these

cells was further corroborated as seen from the extracellular release of HMGB1, a protein marker for necrosis. The release of HMGB1 specifically during necrotic cell death following loss of membrane integrity have been well documented by numerous studies (Evankovich *et al*., 2010, Raucci *et al*., 2007, Scaffidi *et al*., 2002, Yang *et al*., 2007). In apoptotic cells, HMGB1 is deacetylated and retained within the chromatin in the nuclei even upon compromised membrane integrity such as during late apoptosis or secondary necrosis (Evankovich *et al*., 2010, Scaffidi *et al*., 2002). In contrast, during necrosis, HMGB1 is hyperacetylated and translocate from the nucleus to the cytosol, which then passively leaks into the extracellular space upon loss of membrane integrity, contributing to inflammatory responses (Evankovich *et al*., 2010, Yang *et al*., 2007). Cellular contents such as HMGB1, ATP, DNA fragments and mitochondrial contents belongs to a family of intracellular molecules known as Damage-associated molecular patterns (DAMPs) which are immunogenic in extracellular environment or may function as alarmins or cytokines which contributes to inflammatory response (Oppenheim and Yang, 2005, Rock and Kono, 2008).

We have previously reported that peptidyl-methylketones such as z-VAD-FMK and z-FA-FMK are able to deplete intracellular GSH in activated T cells, causing oxidative stress which was inhibited by low molecular weight thiols such GSH, NAC and L-cysteine (Rajah and Chow, 2014; Rajah and Chow, 2015). Interestingly, z-L-CMK toxicity was also completely blocked by NAC suggesting that this peptidyl-CMK was also able to induce oxidative stress in in Jurkat cells. Indeed, z-L-CMK was able to deplete the intracellular GSH level in Jurkat T cells with a concomitant increased in

ROS. Oxidative stress have been shown to play important role in the induction of apoptosis or necrosis frequently, depending on the severity of the insult, which often mediated through the depletion of GSH pools coupled by an increase in ROS (Chandra *et al*., 2000, Orrenius, 2007, Tan *et al*., 1998). The mitochondrion is the main site of cellular respiration as well as the production of ROS such as superoxide anions, hydroxyl radical and hydrogen peroxides. The production of oxygen radicals is attributed to the respiratory chain, exogenous ROS, and cytotoxic insults (Kannan and Jain, 2000). Excessive ROS causes damage to vital cellular components and macromolecules, such as the mitochondria which leads to the collapse of MMP and the release of cytochrome c (Kannan and Jain, 2000, Stridh *et al*., 1998). The released cytochrome c may then take part in the induction of apoptosis by subsequently triggering the caspase activation cascade of the apoptotic intrinsic pathway (Fulda and Debatin, 2006, Hengartner, 2000, Siegel, 2006). However, it remains unclear whether z-L-CMK is able to reacts with intracellular GSH directly causing its depletion which further leads to accumulation of ROS.

In summary, our results have shown that the aminopeptidase inhibitor, z-L-CMK is toxic and readily induces cell death in human Jurkat T cells. Dose-response studies revealed that lower concentration of z-L-CMK readily induces apoptosis while higher concentration of z-L-CMK causes necrosis. Despite having many of the hallmarks of apoptosis, the nuclear morphological changes in z-L-CMK-induced apoptosis were atypical and no DNA fragmentation was observed. This suggests that z-L-CMK may also inhibit downstream processes involved in DNA fragmentation and condensation.

We have also demonstrated that z-L-CMK-induced cell death is mediated via oxidative stress through the depletion of intracellular GSH and accumulation of ROS. Collectively, these results suggest that z-L-CMK possess a potent toxic side effect and careful consideration must be exercised when using it as a specific enzyme inhibitor in cells.





**Figure legends**

**Figure 1. Effect of z-L-CMK on cell viability in Jurkat T cells.** Jurkat T cells were treated with various concentrations of z-L-CMK and the cell viability was determined at different time points using the MTS assay. The results represent the means ± SEM from three independent experiments.

**Figure 2. Effect of z-L-CMK on annexin V-FITC binding and PI uptake in Jurkat T cells.** Cells were treated with various concentrations of z-L-CMK for 6h. Following treatment, the treated cells were stained with annexin V-FITC and PI prior to flow cytometry analysis as described in Materials and methods. The results represent the means ± SEM from three independent experiments.

**Figure 3. Effect of z-L-CMK on Jurkat T cell MMP.** Cells were treated with z-L-CMK (10μM or 50μM) for different time points where indicated. Following treatments, the treated cells were incubated with TMRE prior to flow cytometry analysis as outlined in the Materials and Methods. The results represent the mean fluorescence intensity ± SEM from three independent experiments.

**Figure 4. Effect of z-L-CMK on nuclear morphological changes and DNA in Jurkat T cells.** Cells were treated with 10μM z-L-CMK or 1μM of STS for 6h, fixed and stained with Hoechst 33342 dye as described in Materials and Methods. The nuclear morphological changes (**A-C**) were examined under 400x magnification using fluorescence microscopy and 200 cells were scored for each treatments (**D**). The results represent the means ± SEM from three independent experiments. DNA fragmentation (**E**) was resolved using 2% agarose gel electrophoresis using DNA extracted from treated Jurkat T cells.

**Figure 5. Role of caspases in z-L-CMK-mediated cell death in Jurkat cells.** Cells were treated with various concentrations of z-L-CMK for 6h and cell lysates were prepared and assayed for caspase-3 activity (A). Cells treated with staurosporine (STS) serve as positive control. In (B) and (C), the cells were treated with 10μM and 50μM of z-L-CMK, respectively, for 6h either alone or in the presence of various concentrations of z-VAD-FMK. The results represent the means ± SEM from three independent experiments. RFU (relative fluorescence units).

**Figure 6. The effect of z-L-CMK on the activation of caspases and cleavage of PARP in Jurkat T cells.** Cells were treated with z-FA-CMK (10μM or 50μM) for 6h in the presence or absence of z-VAD-FMK (50μM). Following treatment, caspase activation and cleavage of PARP were examined using Western blotting as described in the Materials and methods. Staurosporine treated cells served as a positive control for

apoptosis in Jurkat T cells. Results are one representative of at least three independent experiments.

**Figure 7. Immunodetection of HMGB1 protein released from z-L-CMK-treated Jurkat T cells.** Cells were treated with various concentration of z-L-CMK for 6h and the culture supernatants were filtered onto nitrocellulose membrane in a dot blot apparatus using vacuum. Immunodetection of HMGB1 in the membrane was carried out as described in materials and methods. (**A**) Dot blot of culture supernatants derived from z-L-CMK treated cells. Results are one representative of at least three separate experiments. (**B**) Dot blot membrane images were captured and the relative signal intensity for HMGB1 protein was analyzed using LI-COR C-DiGit® Blot Scanner. The results are the means ± SEM of the relative intensity of the HMGB1 protein released from z-L-CMK-treated cells from three independent experiments, where * indicates $p < 0.05$ versus control. Freeze thaw (FT) cell lysates were used as positive controls.

**Figure 8. The effect of NAC on z-L-CMK-induced cell death in Jurkat T cells.** Cells were treated with various concentrations of z-L-CMK in the presence and absence of NAC (1mM) for 6h and the cell viability determined using the MTS assay. The results represent the means ± SEM from three independent experiments.

**Figure 9. The effect of z-L-CMK on intracellular GSH and ROS levels in Jurkat T cells.** Cells were incubated with z-L-CMK (10µM or 50µM) for various time points where indicated and the intracellular GSH levels (A) and ROS accumulation (B) were

determined using the fluorescent dye MCB and DHE probes, respectively as outlined in the Materials and Methods. The results represent the means ± SEM from three independent experiments.

**References**

Angliker, H., Wikstrom, P., Rauber, P. & Shaw, E. 1987. The synthesis of lysylfluoromethanes and their properties as inhibitors of trypsin, plasmin and cathepsin B. *Biochem J,* 241**,** 871-5.

Birch, P. L., EL-Obeid, H. A. & Akhtar, M. 1972. The preparation of chloromethylketone analogues of amino acids: Inhibition of leucine aminopeptidase. *Archives of Biochemistry and Biophysics,* 148**,** 447-451.

Chandra, J., Samali, A. & Orrenius, S. 2000. Triggering and modulation of apoptosis by oxidative stress. *Free Radic Biol Med,* 29**,** 323-33.

Degterev, A., Boyce, M. & Yuan, J. 2003. A decade of caspases. *Oncogene,* 22**,** 8543-8567.

Ding, W.-X., Shen, H.-M. & Ong, C.-N. 2000. Critical Role of Reactive Oxygen Species and Mitochondrial Permeability Transition in Microcystin-Induced Rapid Apoptosis in Rat Hepatocytes. *Hepatology,* 32**,** 547-555.

Enari M[1], Sakahira H, Yokoyama H, Okawa K, Iwamatsu A, Nagata S. 1998. A caspase-activated DNase that degrades DNA during apoptosis, and its inhibitor ICAD. *Nature*, 391, 43-50.

Evankovich, J., Cho, S. W., Zhang, R., Cardinal, J., Dhupar, R., Zhang, L., Klune, J. R., Zlotnicki, J., Billiar, T. & Tsung, A. 2010. High mobility group box 1 release from

hepatocytes during ischemia and reperfusion injury is mediated by decreased histone deacetylase activity. *J Biol Chem,* 285**,** 39888-97.

Fulda, S. & Debatin, K. M. 2006. Extrinsic versus intrinsic apoptosis pathways in anticancer chemotherapy. *Oncogene,* 25**,** 4798-4811.

Gillibert, M., Dehry, Z., Terrier, M., EL Benna, J. & Lederer, F. 2005a. Another biological effect of tosylphenylalanylchloromethane (TPCK): it prevents p47 phox phosphorylation and translocation upon neutrophil stimulation. *Biochemical Journal,* 386**,** 549-556.

Gillibert, M., Dehry, Z., Terrier, M., El Benna, J. & Lederer, F. 2005b. Another biological effect of tosylphenylalanylchloromethane (TPCK): it prevents p47phox phosphorylation and translocation upon neutrophil stimulation. *Biochem J,* 386**,** 549-56.

Ha, K.-H., Byun, M.-S., Choi, J., Jeong, J., Lee, K.-J. & Jue, D.-M. 2009. N-tosyl-L-phenylalanine chloromethyl ketone inhibits NF-kB activation by blocking specific cysteine residues of IkB kinase B and p65/RelA. *Biochemistry,* 48**,** 7271-7278.

Hengartner, M. O. 2000. The biochemistry of apoptosis. *Nature,* 407**,** 770-776.

Johnson, V. L., Ko, S. C., Holmstrom, T. H., Eriksson, J. E. & Chow, S. C. 2000. Effector caspases are dispensable for the early nuclear morphological changes during chemical-induced apoptosis. *J Cell Sci,* 113 ( Pt 17)**,** 2941-53.

Kamencic, H., Lyon, A., Paterson, P. G. & Juurlink, B. H. 2000. Monochlorobimane fluorometric method to measure tissue glutathione. *Anal Biochem,* 286**,** 35-7.

Kannan, K. & Jain, S. K. 2000. Oxidative stress and apoptosis. *Pathophysiology,* 7**,** 153-163.

Kim, H., Lee, H. S., Chang, K. T., Ko, T. H., Baek, K. J. & Kwon, N. S. 1995. Chloromethyl ketones block induction of nitric oxide synthase in murine macrophages by preventing activation of nuclear factor-kappa B. *J Immunol,* 154**,** 4741-8.

Krantz, A., Copp, L. J., Coles, P. J., Smith, R. A. & Heard, S. B. 1991. Peptidyl (acyloxy)methyl ketones and the quiescent affinity label concept: the departing group as a variable structural element in the design of inactivators of cysteine proteinases. *Biochemistry,* 30**,** 4678-87.

Lawrence, C. P., Kadioglu, A., Yang, A. L., Coward, W. R. & Chow, S. C. 2006. The cathepsin B inhibitor, z-FA-FMK, inhibits human T cell proliferation in vitro and modulates host response to pneumococcal infection in vivo. *J Immunol,* 177**,** 3827-36.

Liow, K. Y. & Chow, S. C. 2013. The cathepsin B inhibitor, z-FA-CMK is toxic and readily induced cell death in human T lymphocytes. *Toxicol Appl Pharmacol,* 272**,** 559-67.

Liu, X., Zou, H., Slaughter, C., Wang, X. 1997. DFF, a heterodimeric protein that functions downstream of caspase-3 to trigger DNA fragmentation during apoptosis. Cell, 89,175-184.

Oppenheim, J. J. & Yang, D. 2005. Alarmins: chemotactic activators of immune responses. *Curr Opin Immunol,* 17**,** 359-65.

Orrenius, S. 2007. Reactive oxygen species in mitochondria-mediated cell death. *Drug Metab Rev,* 39**,** 443-55.

Owusu-Ansah, E., Yavari, A. & Banerjee, U. 2008. A protocol for _in vivo_ detection of reactive oxygen species.

Perez-G, M., Cortes, J. R., Rivas, M. D., Masa, F. & Zamorano, J. 2008. Treatment of cells with n-alpha-tosyl-l-phenylalanine-chloromethyl ketone induces the proteolytic loss of STAT6 transcription factor. *Molecular Immunology,* 45**,** 3896-3901.

Powers, J. C., Aagian, J. L., Ekici, O. D. & James, K. E. 2002. Irreversible inhibitors of serine, cysteine, and threonine proteases. *Chem Rev,* 102**,** 4639-750.

Rajah, T. & Chow, S. C. 2014. The inhibition of human T cell proliferation by the caspase inhibitor z-VAD-FMK is mediated through oxidative stress. *Toxicol Appl Pharmacol,* 278**,** 100-6.

Rajah, T. & Chow, S. C. 2015. Suppression of human T cell proliferation mediated by the cathepsin B inhibitor, z-FA-FMK is due to oxidative stress. PLoS ONE 10(4):e0123711

Rauber, P., Angliker, H., Walker, B. & Shaw, E. 1986. The synthesis of peptidylfluoromethanes and their properties as inhibitors of serine proteinases and cysteine proteinases. *Biochem J,* 239**,** 633-40.

Raucci, A., Palumbo, R. & Bianchi, M. E. 2007. HMGB1: a signal of necrosis. *Autoimmunity,* 40**,** 285-9.

Rock, K. L. & Kono, H. 2008. The inflammatory response to cell death. *Annu Rev Pathol,* 3**,** 99-126.

Sakahira, H., Enari, M., Nagata, S. 1998. Cleavage of CAD inhibitor in CAD activation and DNA degradation during apoptosis. Nature, 391,96-99.

Scafidi, P., Misteli, T. & Bianchi, M. E. 2002. Release of chromatin protein HMGB1 by necrotic cells triggers inflammation. *Nature,* 418**,** 191-195.

Schoellmann, G. A. S., E. 1962. A new method for labelling the active center of chymotrysin. *Biochemical and Biophysical Research Communications,* 7**,** 36-40.

Shaw, E., Angliker, H., Rauber, P., Walker, B. & Wikstrom, P. 1986. Peptidyl fluoromethyl ketones as thiol protease inhibitors. *Biomed Biochim Acta,* 45**,** 1397-403.

Siegel, R. M. 2006. Caspases at the crossroads of immune-cell life and death. *Nat Rev Immunol,* 6**,** 308-17.

Stridh, H., Kimland, M., Jones, D. P., Orrenius, S. & Hampton, M. B. 1998. Cytochrome c release and caspase activation in hydrogen peroxide- and tributyltin-induced apoptosis. *FEBS Lett,* 429**,** 351-5.

Tan, S., Sagara, Y., Liu, Y., Maher, P. & Schubert, D. 1998. The regulation of reactive oxygen species production during programmed cell death. *J Cell Biol,* 141**,** 1423-32.

Taylor, R. C., Cullen, S. P. & Martin, S. J. 2008. Apoptosis: controlled demolition at the cellular level. *Nat Rev Mol Cell Biol,* 9**,** 231-41.

Van Engeland, M., Nieland, L. J., Ramaekers, F. C., Schutte, B. & Reutelingsperger, C. P. 1998. Annexin V-affinity assay: a review on an apoptosis detection system based on phosphatidylserine exposure. *Cytometry,* 31**,** 1-9.

Weis, M., Schlegel, J., Kass, G. E. N., Holmstrom, T. H., Peters, I., Eriksson, J. E., Orrenius, S. & Chow, S. C. 1995. Cellular events in Fas/APO-1-mediated apoptosis in JURKAT T lymphocytes. 219**,** 699-708.

Wolf, B.B., Schuler, M., Echeverri, F., Green, D.R. 1999. Caspase-3 is the primary activator of apoptotic DNA fragmentation via DNA fragmentation factor-45/inhibitor of caspase-activated DNase inactivation.

Yang, D., Chen, Q., Yang, H., Tracey, K. J., Bustin, M. & Oppenheim, J. J. 2007. High mobility group box-1 protein induces the migration and activation of human dendritic cells and acts as an alarmin. *Journal of Leukocyte Biology,* 81**,** 59-66.

Zhang, G., Gurtu, V., Kain, S. R. & Yan, G. 1997. Early detection of apoptosis using a fluorescent conjugate of annexin V. *Biotechniques,* 23**,** 525-31.

Figure 1

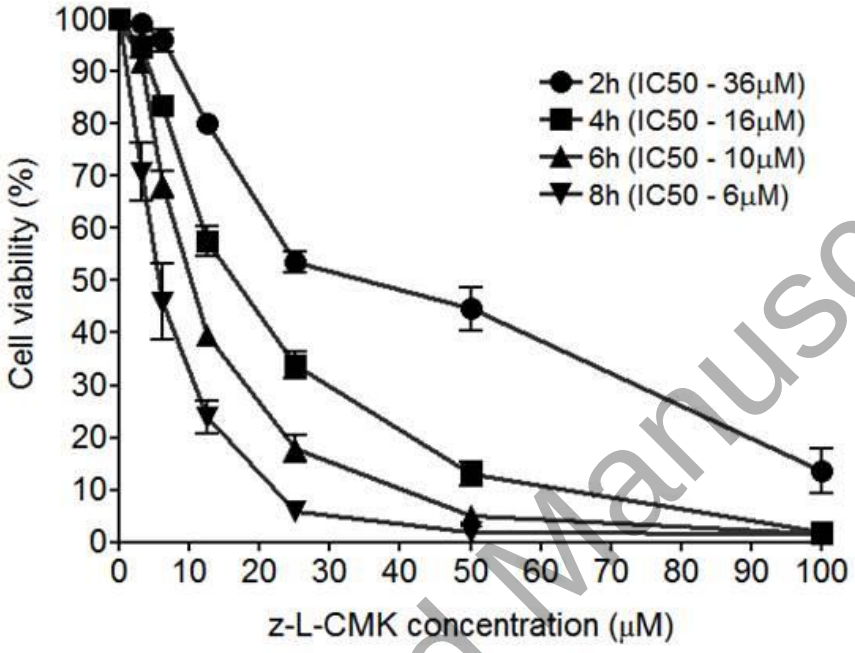

Figure 2

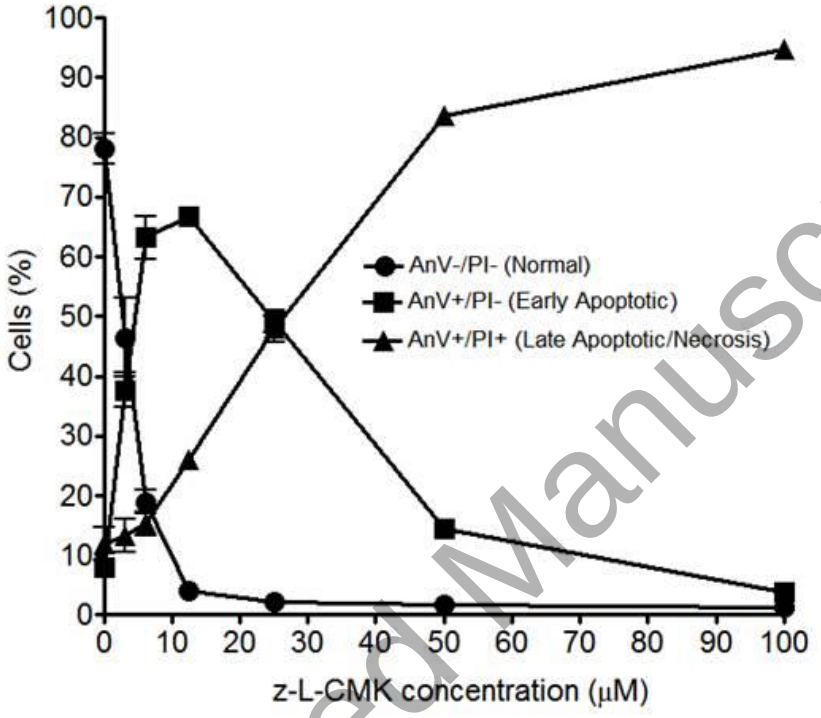

Figure 3

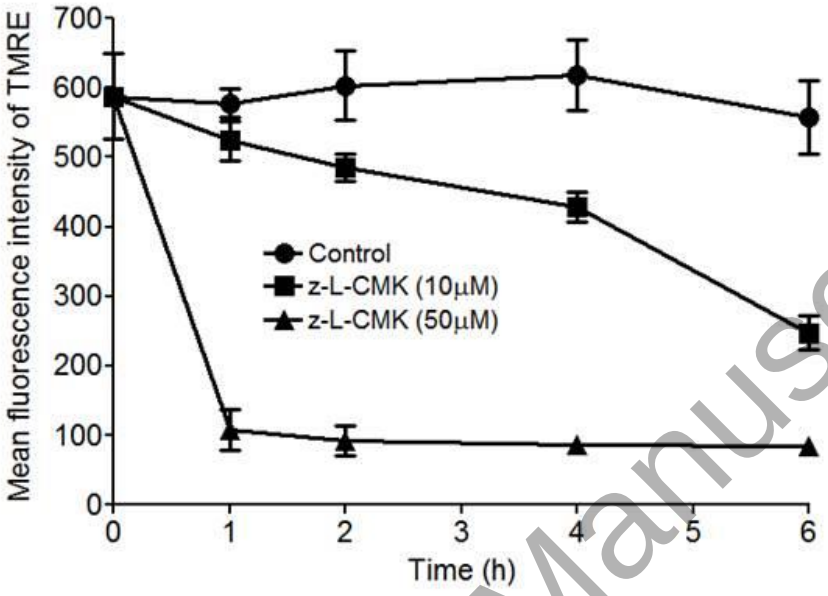

Figure 4

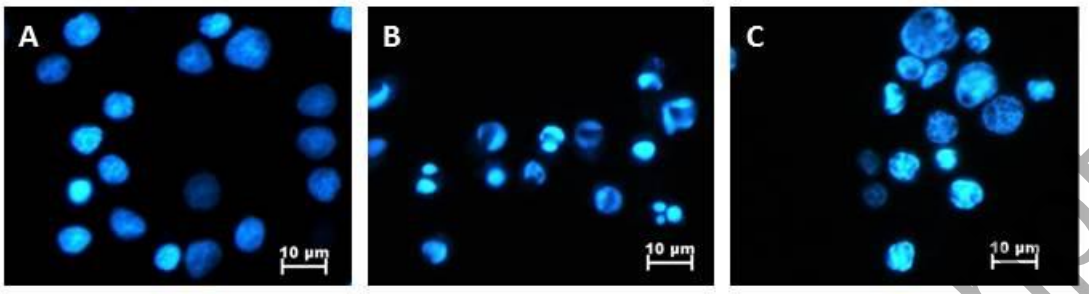


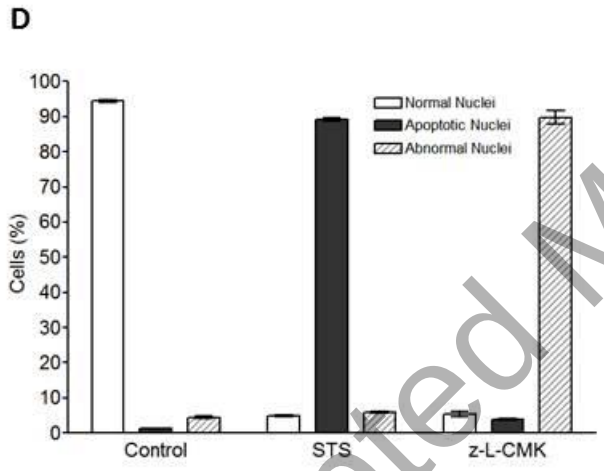


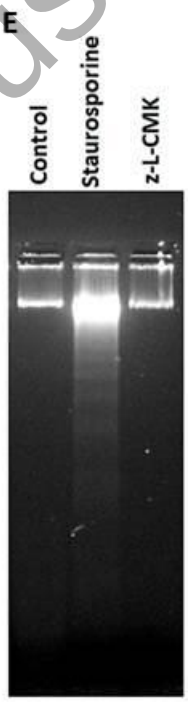

Figure 5

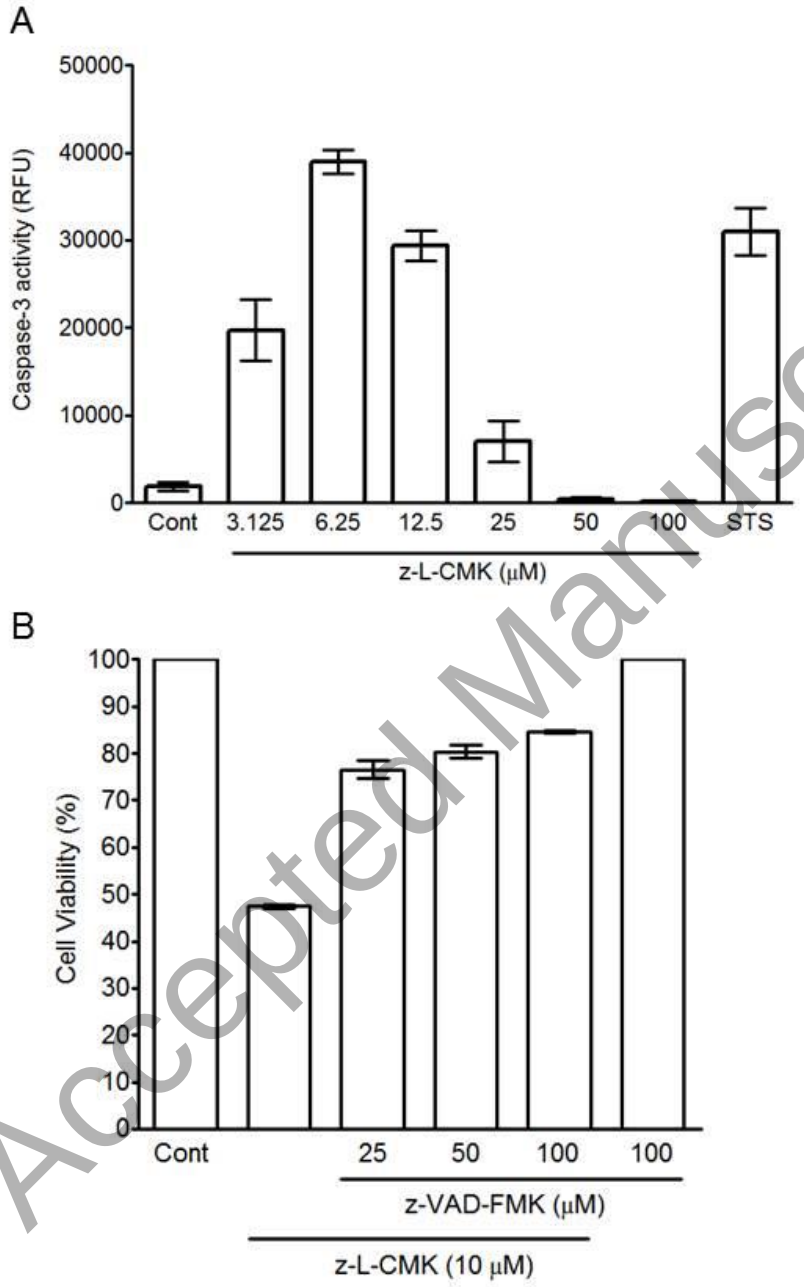

Figure 5

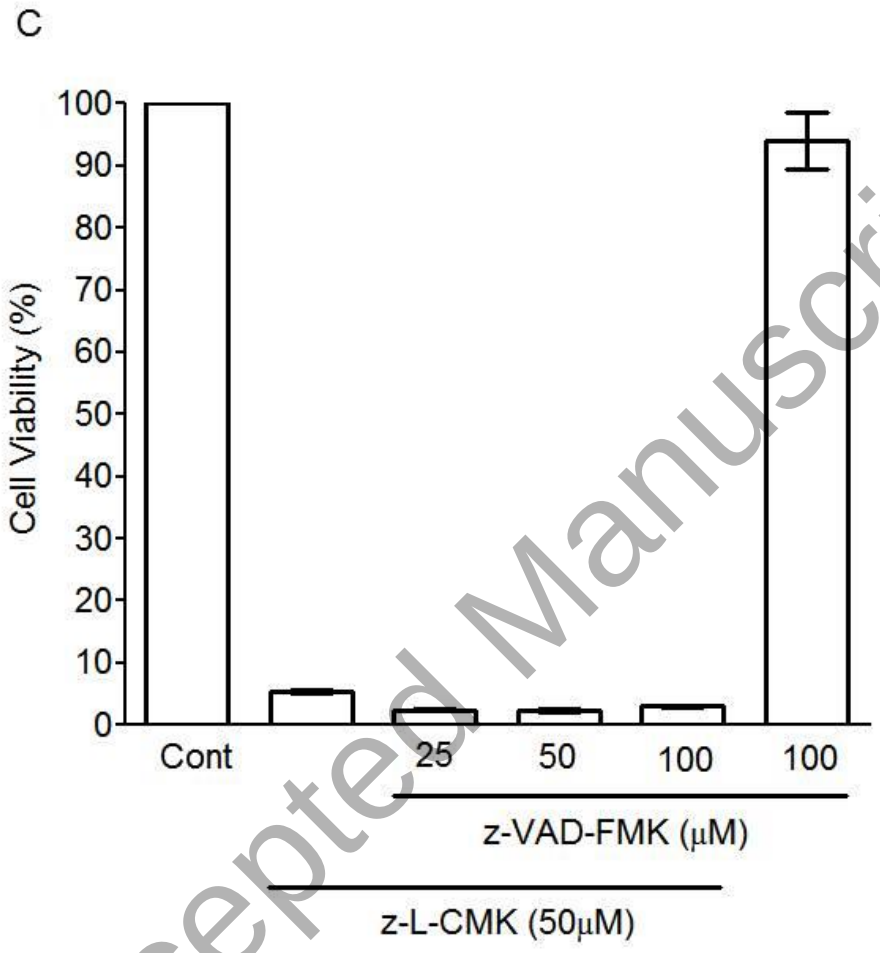

Figure 6

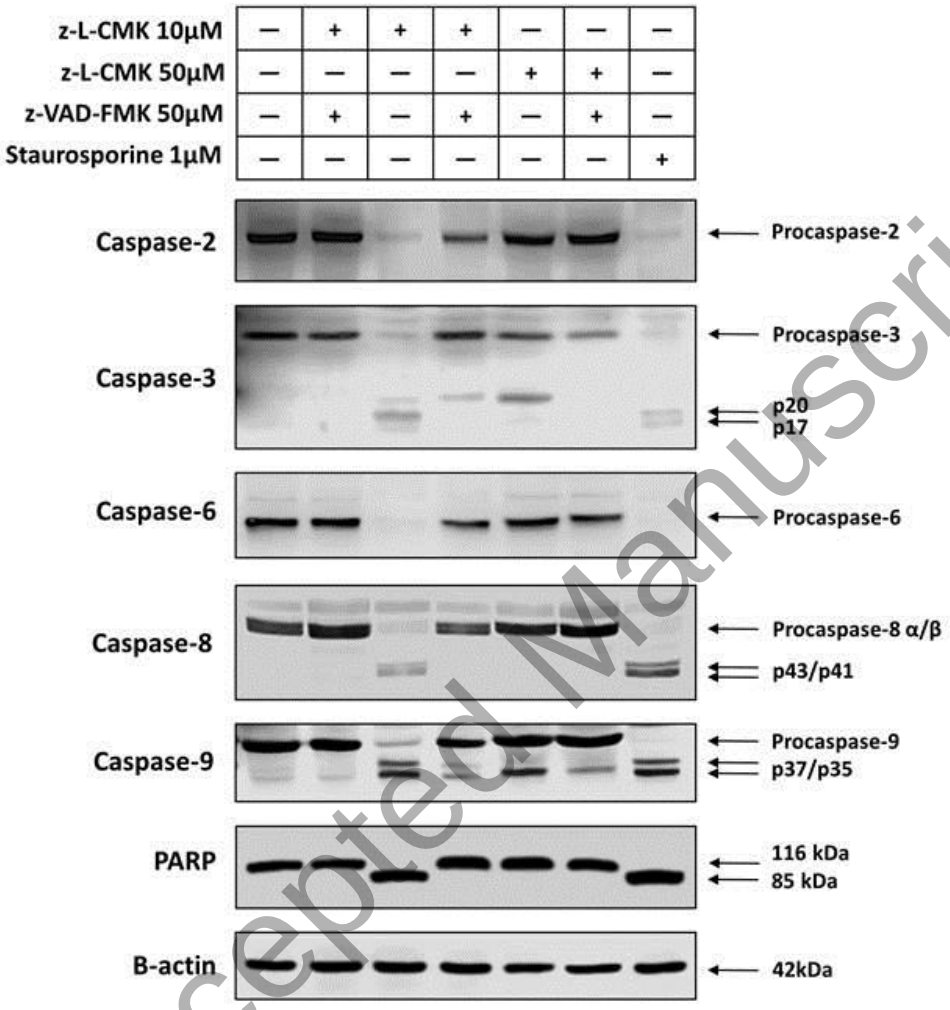

Figure 7

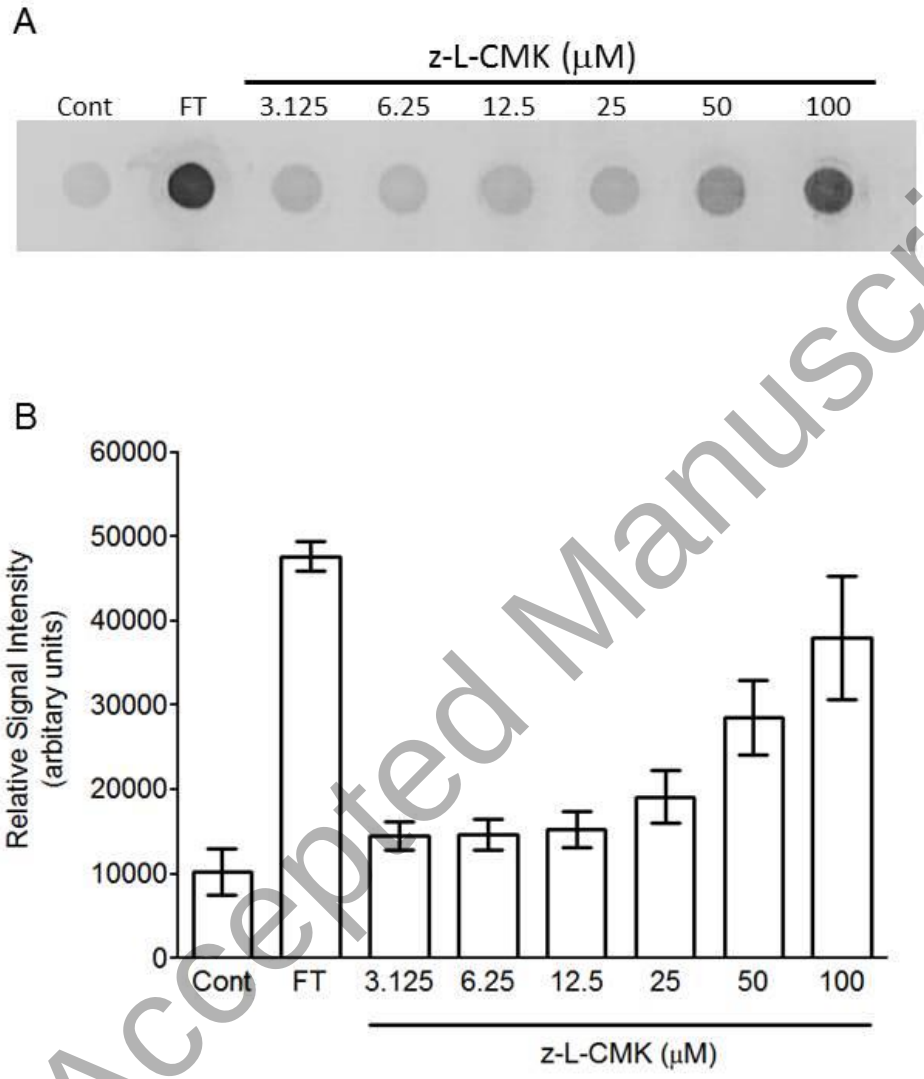

Figure 8

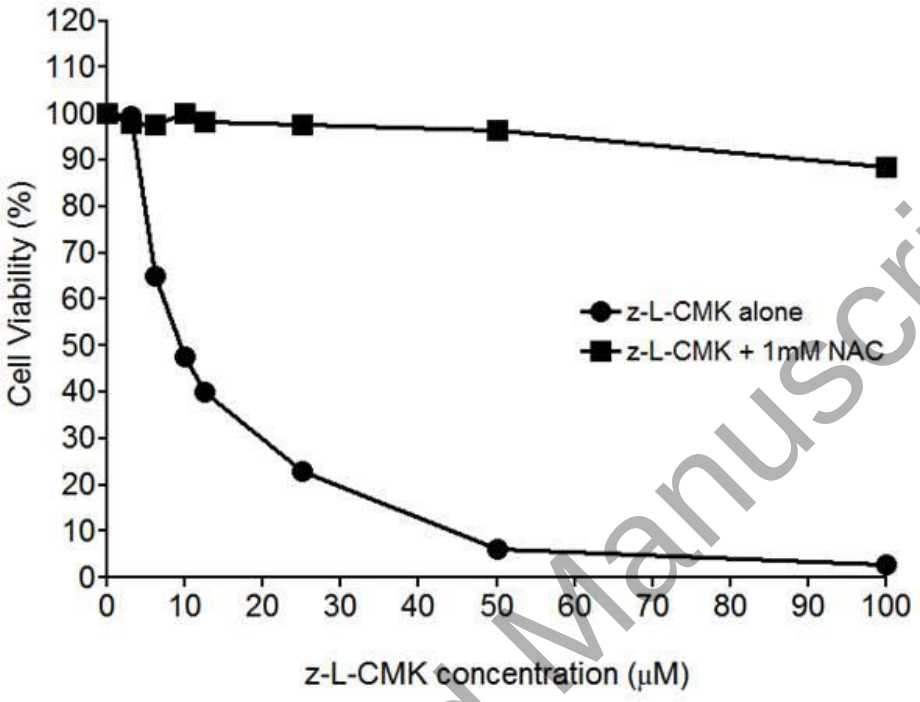

Figure 9